Challenge Journal of CONCRETE RESEARCH LETTERS

Research Article

Structural behavior of lightweight composite ferrocement plates

Yousry B. I. Shaheen [a], Noha Gamal Rady [a], Fatma M. Eid [a,*]

[a] *Department of Civil Engineering, Menoufia University, 32511 Shebin El-Kom, Menofia, Egypt*

ABSTRACT

Ferrocement is a reinforced cementitious composite consisting of layers of wire mesh or small-diameter steel rods embedded in cement mortar. Its structural efficiency depends mainly on reinforcement geometry and distribution rather than on material quantity alone. This study examines the flexural behavior of ten lightweight ferrocement plates reinforced with different mesh types, namely welded metal mesh, Gavazzi mesh, and Tenax mesh. All plate specimens had dimensions of 1200 mm × 500 mm × 120 mm and contained corrugated foam panels embedded at the mid-depth. Steel mesh with a wire diameter of 5.5 mm was provided at the top and bottom as the main reinforcement. The load-deflection response, cracking behavior, ductility, energy absorption, and overall flexural performance were evaluated to determine the effect of mesh type and mesh-layer arrangement on structural efficiency. The results showed that plates reinforced with four layers of welded metal mesh achieved the best ultimate strength and crack resistance. These plates reached ultimate and service loads that were 34% and 48.88% higher, respectively, than those of the control specimen without additional mesh. In contrast, the plate reinforced with one additional layer of Gavazzi mesh showed the highest energy absorption among all specimens, with a value 75.9% higher than that of the control specimen. Increasing the number of mesh layers improved cracking load, service load, ultimate load, and energy absorption. Welded metal mesh also outperformed Tenax mesh in energy absorption, making it preferable for structural elements requiring high toughness and resilience.

ARTICLE INFO

Article history:
Received – January 3, 2026
Revision requested – February 9, 2026
Revision received – March 25, 2026
Accepted – March 30, 2026

Keywords:
Lightweight concrete
Composite plates
Ferrocement
Flexural behavior
Welded metal mesh
Gavazzi mesh
Tenax mesh

Citation: Shaheen YBI, Rady NG, Eid FM (2026). Structural behavior of light weight composite ferrocement plates. *Challenge Journal of Concrete Research Letters*, 17(2), 177–191.

1. Introduction

Ferrocement is produced by layering continuous wire meshes that are tied together, with reinforcement ratios that may reach approximately 8%. The mortar cover over the meshes is typically between 3 and 5 mm, which promotes a uniform distribution of reinforcement. This configuration improves material homogeneity and enhances mechanical properties such as tensile strength, flexural performance, impact resistance, and crack control. The interconnected wire meshes are filled with cement mortar, forming a dense composite material that can be molded into thin, lightweight sections without losing structural integrity.

In ferrocement members, the structural response is strongly influenced by the mortar matrix, reinforcement ratio, and the type, stiffness, geometry, and distribution of the reinforcing mesh. Recent studies on ferrocement beams have shown that metallic and non-metallic mesh configurations can significantly affect first cracking load, ultimate load, ductility, energy absorption, crack distribution, and load-to-weight efficiency, particularly when material-efficient sections such as beams with openings or lightweight cores are considered (Hekal et al. 2024; Shaheen et al. 2024).

Shaheen et al. (2023a) studied the structural performance of ferrocement beams with longitudinal perforations filled with lightweight concrete. The experimental

* *Corresponding author*. E-mail address: fatma_elzahraa2002@yahoo.com (F. M. Eid)
ISSN: 2548-0928 / DOI: https://doi.org/10.20528/cjcrl.2026.02.008

program included two normal-weight concrete (NWC) beams and ten ferrocement (FC) beams with lightweight cores reinforced with welded steel mesh used as shear reinforcement and tested under three-point bending. The lightweight core concrete contained aerated autoclaved brick waste and expanded polystyrene. Compared with the control NWC beam, the FC beams with different filler materials and welded steel meshes instead of conventional stirrups increased ultimate load by 36.6-107.3%, ultimate deflection by 6-272%, and ductility by 89-1155%.

Qureshi et al. (2023) conducted four-point bending tests on 16 simply supported ferrocement panels measuring 1000 mm × 450 mm to evaluate the flexural performance of panels containing SBR latex. The results indicated that latex and polypropylene (PP) fibers mainly affected the initial stiffness and had limited influence on the final load. The control specimens had a lower peak load than specimens reinforced with welded iron mesh, whereas specimens with PVC mesh showed greater flexural toughness than those with welded iron mesh. This is consistent with recent observations that metallic meshes generally provide higher stiffness and strength contribution, whereas non-metallic meshes such as Gavazzi, Tensar, or polymer-based grids may improve crack distribution, deformation capacity, and energy absorption depending on their tensile stiffness, elongation capacity, and bond with the mortar matrix (Hekal et al. 2024). The PVC plastic mesh specimens also exhibited a smeared cracking pattern, indicating greater ductility than the iron mesh specimens.

Several additional studies have investigated ferrocement and ferrocement-related systems in different structural applications. These include lightweight ferrocement box columns, geopolymer ferrocement beams, reinforced concrete beams strengthened with U-shaped ferrocement jackets, sustainable high-performance mortar with natural sisal fibers, fiber-reinforced ferrocement beams under monotonic and repeated loading, ferrocement panels under flexural and impact loads, lightweight panels with expanded perlite, sandwich panel slabs under shear, ferrocement I-beams, composite ferrocement-concrete plates, and voided ferrocement channel sections (Eltaly et al. 2023; El-Sayed et al. 2023; Rajguru and Patkar 2022; Dawood et al. 2021; Naveen and Suresh 2020; Murali et al. 2020; Madadi et al. 2018; Shaheen et al. 2016; Acma et al. 2015; Shaheen et al. 2013; Rao et al. 2008). Collectively, these studies confirm the ability of ferrocement systems to improve strength, stiffness, cracking behavior, ductility, energy absorption, and weight efficiency.

Similarly, studies on ferrocement beams with web or circular openings have indicated that material reduction in selected regions may improve structural efficiency, but it can also alter stress flow, crack propagation, stiffness, ductility, and energy absorption depending on the opening configuration and mesh type (Hekal et al. 2024; Shaheen et al. 2024). These findings are directly relevant to lightweight ferrocement systems because reducing self-weight through voids, openings, or lightweight cores requires a balanced assessment of ultimate load, serviceability, deflection response, crack pattern, ductility, energy absorption, and load-to-weight ratio.

Abdel Tawab (2006) developed U-shaped ferrocement permanent formwork as a practical alternative to conventional wooden and metal forms for reinforced concrete beams. Shaheen et al. (2023b) studied ferrocement walls under vertical and horizontal loading. The walls consisted of two thin ferrocement layers reinforced with one, two, three, or four layers of welded wire mesh or expanded steel mesh, with a lightweight extruded foam core. Thirteen lightweight walls with dimensions of 100 mm × 650 mm × 1250 mm were cast and tested until failure, and ABAQUS finite element analysis was also performed. The results showed that walls reinforced with expanded wire meshes performed better than walls reinforced with welded wire meshes. Energy absorption increased by 40% in the specimens reinforced with expanded wire meshes compared with the corresponding welded wire mesh specimens.

Based on this review, the present study examines the structural behavior of ferrocement plates reinforced with different mesh types. The study also evaluates the effects of mesh type, number of mesh layers, and combinations of different mesh systems, together with the use of corrugated foam panels to reduce plate weight.

Although previous studies have examined ferrocement beams with openings and highlighted the effects of mesh type, opening configuration, and load-to-weight efficiency, limited information is available on lightweight ferrocement plates incorporating corrugated foam cores with different metallic and non-metallic mesh systems. Therefore, this study extends the existing ferrocement literature from beam-type members with openings to plate-type lightweight composite elements by focusing on flexural performance, cracking behavior, ductility, energy absorption, and structural efficiency.

This research introduces a new integration of ferrocement and corrugated foam-core systems for developing ultra-lightweight and sustainable structural elements. By evaluating welded, Gavazzi, and Tenax meshes, the study assesses the influence of hybrid reinforcement and bond-slip mechanisms in thin composite plates. The use of corrugated foam panels reduces self-weight without compromising flexural integrity, thereby providing a resource-efficient model for building envelope applications. The study also quantifies a 75.9% increase in energy absorption when Gavazzi mesh is used, indicating improved flexural toughness and energy dissipation capacity under monotonic loading. Overall, the proposed system supports sustainable construction by reducing concrete volume and improving thermal resistance within a single lightweight structural unit.

2. Experimental Materials

This section describes the materials used to develop the mortar mix and fabricate the tested plates, including cement, fine aggregate, water, superplasticizer, polypropylene fibers, silica fume, reinforcing meshes, and corrugated foam panels. The materials were evaluated in accordance with ASTM, BS, and ECP standards to determine their physical and mechanical properties, and they were also visually inspected for cleanliness and overall quality.

2.1. Cement

Ordinary Portland cement (OPC), CEM I 42.5 N, was used in the experimental program, as shown in Fig. 1. The cement was supplied by El-Sewedy Cement Company. The chemical composition of the cement is presented in Table 1 according to the manufacturer's data. As shown in Table 2, the cement satisfied the physical and chemical requirements of the Egyptian standard specification ESS 4756-1/2022.

Fig. 1. Cement used in the mixes.

Table 1. Chemical composition of OPC CEM I / 42.5 N.

Constituents	Concentration in weight (%)	Constituents	Concentration in weight (%)
Silica as SiO_2	19.8	Lime saturation factor	100.4
Alumina as AL_2O_3	5.6	Lime combination factor	98.9
Iron as FeO_3	2.4	Silica ratio	2.48
Potassium as k_2O	0.58	Alumina ratio	2.33
Calcium as CaO	65.9	Tricalcium Cilicate (C_3S)	65.1
Sodium as Na_2O	0.29	Dicalcium Cilicate (C_2S)	7.6
Sulphur as SO_3	2.8	Tricalcium Aluminate (C_3A)	10.8
Loss in ignition	1.2	Insoluble residue	0.4

Table 2. Characteristics of cement used.

Test description		Test results	E.S.S. 4756-1/2022 Egyptian specification limits
Setting time (Vicat test) Initial Final		hour: min 1: 55 4: 10	 Not less than 60 min Not more than 10 h
The soundness of cement (Le Chatelier test)		4 mm	Not more than 10mm
The fineness of cement, percentage retained on the standard 0.09 mm sieve by weight		7%	Not more than 10%
Specific surface area		3140 cm^2/g	Not less than 2800 cm^2/g
Compressive strength of cement mortar (MPa)	2 days	14	≥10
	28 days	48	≥42.5

2.2. Fine aggregate

Natural siliceous sand was used as the fine aggregate. The sand was free from impurities and had a specific gravity of 2.6 and a fineness modulus of 2.91. These properties comply with ESS 1109/2008 and ICS 91.100.10 EN 12620/2002+A1. The properties of the sand are presented in Table 3, while its grading is shown in Table 4 and Fig. 2.

Table 3. Properties of fine aggregate used.

Property	Test results for sand
Specific gravity (S.S.D)	2.6
Unit weight	1.7 t/m^3
Fineness modulus	2.91
Clay, silt, and fine dust	2% (by weight)
Chloride	0.03% (by weight)

Table 4. Results of sieve analysis test for fine aggregate.

Sieve diameter (mm)	4.75	2.36	1.18	0.60	0.30	0.15
% Passing	100	92.8	82.6	37.7	9.50	0
% Passing (E.S.S. 1109/2008) (Medium Zone)	100	60–100	30–90	15–45	5–40	0

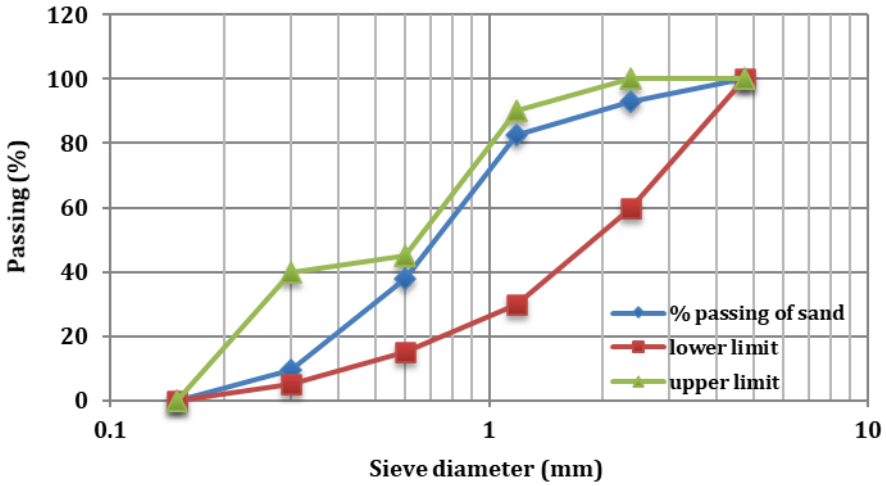

Fig. 2. Grading curve of sand used.

2.3. Water

Clean potable water, free from impurities, was used for mixing and curing the plates in accordance with ECP 203/2020.

2.4. Superplasticizer

The superplasticizer used in this study was a high-range water reducer (HRWR) designed to improve mix workability. As shown in Fig. 3, this additive was produced by Sika Group and marketed as Sika ViscoCrete 3425. It complies with ASTM C494, Types A and F. The product reduces mixing time by improving polymer dispersion, enhances water resistance, improves bonding between new and old concrete or plaster, increases strength properties, and helps minimize shrinkage and cracking. Its relative density is 1.02 ± 0.01 at 25 °C.

2.5. Polypropylene fibers

PP 300-e3 polypropylene fibers were used in the concrete mixtures, as shown in Fig. 4. These fibers are available in the Egyptian market and were added to improve the properties of the mortar. The recommended dosage was 900 g/m^3, as specified by the manufacturer.

2.6. Silica fume

Silica fume, or microsilica, is a non-crystalline form of silicon dioxide. As shown in Fig. 5, it is an ultrafine powder produced during the manufacture of silicon and ferrosilicon alloys. It contains spherical particles with an average size of approximately 150 nm. Its primary use is as a pozzolanic material in high-performance concrete. The silica fume used in this study had a specific gravity of 2.63, and the recommended dosage was 7-10% of the cement weight.

2.7. Reinforcement

2.7.1. Welded steel bars

A mesh panel made of welded steel bars, with dimensions of 500 mm × 1200 mm, openings of 100 mm × 100 mm, and a wire diameter of 5.5 mm, was used as shown in Fig. 6. This product was manufactured in accordance with standard specifications and supplied by Ezz Steel Company, ensuring adequate quality and strength.

Fig. 3. Superplasticizer.

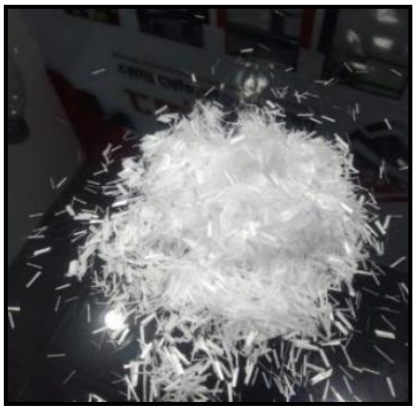

Fig. 4. Polypropylene fibers PP 300-e3.

Fig. 5. Silica fume.

Fig. 6. Welded steel bars used.

2.7.2. Welded metal mesh

Welded metal mesh was used as additional reinforcement together with the welded steel bars in the ferrocement plates. The welded wire mesh consisted of galvanized wires with a diameter of 0.7 mm and openings of 12.5 mm × 12.5 mm, as shown in Fig. 7. The technical specifications and mechanical properties provided by the manufacturer are given in Table 5.

Fig. 7. Welded mesh used.

Table 5. Technical specifications and mechanical properties of welded mesh.

Property	Dimensions	Weight	Modulus of elasticity	Proof stress	Ultimate strength	Ultimate strain	Proof strain
Value	12.5×12.5 mm	430 g/m^2	170 GPa	400 N/mm^2	600 N/mm^2	58.8×10^{-3}	1.17×10^{-3}

2.7.3. Gavazzi mesh

Gavazzi mesh is a fiberglass mesh produced by Gavazzi Company in Italy and is available in the Egyptian market, as shown in Fig. 8. According to the manufacturer, the mesh opening is 8.3 mm × 9.5 mm, the longitudinal cross-section is 1.66 mm × 0.66 mm, and the transverse cross-section is 1.0 mm × 0.5 mm. The mesh has a weight of 222 g/m^2 and a volume fraction of 0.535%. Its longitudinal tensile strength is 32.5 MPa, with an elongation of 5.5%, as presented in Table 6.

2.7.4. Tenax mesh

Tenax mesh is a non-metallic wire mesh known as uniaxial Geogrid TT060 and is made of high-density polyethylene. As shown in Fig. 9, it has an aperture size of 21 mm × 7 mm, a weight of 1.5 kg/m^2, and a volume fraction of 2.04%. The Tenax mesh has a tensile strength of 24.7 MPa at an elongation of 21%. Table 7 presents the technical and mechanical properties of uniaxial Geogrid TT060.

Fig. 8. Gavazzi mesh used.

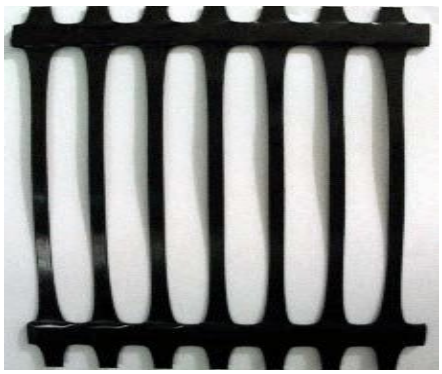

Fig. 9. Tenax mesh used.

Table 6. Technical and mechanical properties of Gavazzi mesh.

Product name	Gavazzi 0225-A
Mesh opening	8.3×9.5 mm
Weight	222 g/m² ± 5%
Modulus of elasticity	72 GPa
Composition	Fiberglass approx. 87% Alkali-resistant finish approx. 13
Tensile resistance	Breaking strength elongation Warp approx. 3200 N/5 cm 5% ± 1 Weft approx. 3200 N/5 cm 5% ± 1

Table 7. Technical and mechanical properties of uniaxial Geogrid TT060.

Technical characteristics	Units	MD values
Tensile strength at 5% strain	kN/m	35
Tensile strength at 5% strain	kN/m	100
Junction strength	kN/m	50
Modulus of elasticity	MPa	100
Flexural stiffness	mg·cm	730.000
Technical characteristics	Units	MD Values

2.7.5. Corrugated foam panels

Corrugated foam panels with a thickness of approximately 40 mm and strengthened with metal wire meshes were obtained from the Egyptian Italian Company for Modern Construction, Cairo, Egypt. As shown in Fig. 10, the panels were subjected to standard laboratory tests by the manufacturer in accordance with the applicable Egyptian standard specifications. The test results are presented in Table 8.

Fig. 10. Corrugated foam panels used.

Table 8. Physical properties extracted from European foam manufacturers.

Description	Value
Mold net dimension	1.20 × 0.80 × 4.0 m
Density	19–21 kg/m³
Compressive strength at 10% deformation (at 20°C)	1.60 kg/cm²
Compressive strength at 10% deformation (at 70°C)	1.20 kg/cm²
Compressive creep strength for 50 years at 2% deformation (20°C)	0.48 kg/cm²
Compressive creep strength for 50 years at 2% deformation (70°C)	0.36 kg/cm²
Tensile strength at 20°C	2.6 kg/cm²
Tensile strength at 70°C	1.8 kg/cm²

3. Experimental Program

Ten ferrocement plates were tested to evaluate their performance under flexural loading. The specimens were cast with dimensions of 1200 mm × 500 mm × 120 mm in accordance with the design, mixing, and curing requirements of the Egyptian Code of Practice (ECP 203/2020). Each specimen consisted of ferrocement plates reinforced at the top and bottom with 1200 mm × 500 mm steel mesh panels having 100 mm × 100 mm openings and a 5.5 mm wire diameter. Additional reinforcement was provided using welded galvanized steel mesh, Gavazzi mesh, and Tenax mesh.

- Group A included four specimens and was used to evaluate the effect of increasing the number of welded steel mesh layers from one to four.
- Group B included three specimens and was used to evaluate the effect of increasing the number of Tenax mesh layers from one to three.
- Group C included two specimens and was used to investigate the performance of Gavazzi mesh and a hybrid Gavazzi-Tenax reinforcement system. One specimen (PC) was kept as the control specimen without additional reinforcement. This specimen matrix enabled a comparative evaluation of ultimate load, ductility, energy absorption, serviceability response, and load-to-weight ratio while keeping the experimental scope consistent with similar recent studies.

The number of mesh layers was limited to four to ensure full mortar infiltration around the corrugated foam core within the 120 mm composite section. Exceeding this limit could create physical barriers, cause internal voids, and reduce bond integrity. Symmetric reinforcement was used on both faces to maintain structural integrity under positive and negative bending during handling and service and to control shrinkage-induced cracks on both sides.

A plain mortar mixture without additives was not included because the study aimed to develop a high-performance mortar capable of meeting the structural demands of 120 mm lightweight slabs. The additives used were already available in the local market. Silica fume acted as a micro-filler and pozzolanic material, increasing compressive strength and improving the interfacial transition zone between the mortar, mesh, and corrugated foam core. Polypropylene fibers were added to enhance tensile strength, control shrinkage cracking, and increase toughness. Together, these materials produced a dense and durable matrix with the flowability required for full infiltration around the foam corrugations, which standard mortar could not provide.

The primary variables were the reinforcement mesh type and the number of additional mesh layers placed at the top and bottom of the plates, as detailed in Table 9. All tests were performed in the construction materials laboratory at Menoufia University, Egypt. Fig. 11 shows the cross-sectional details of all tested plates.

Table 9. Details of the tested specimens.

Group number	Specimen name	Foam with steel wires	Additional mesh reinforcement		Steel mesh
1	PC	One foam layer with a thickness of 40 mm and steel wires (top + bottom) with 3.3 mm thickness	No mesh		steel mesh at top and bottom with 5.5 mm wire diameter
2	PW1		Welded mesh top and bottom	1 layer	
	PW2			2 layers	
	PW3			3 layers	
	PW4			4 layers	
3	PT1		Tenax mesh top and bottom	1 layer	
	PT2			2 layers	
	PT3			3 layers	
4	PG1		Gavazzi mesh top and bottom	1 layer	
	PG1+T1		Gavazzi mesh + Tenax mesh	1 layer + 1 layer	

3.1. Mortar mix design

Mortar quality is one of the most important factors affecting the behavior of ferrocement units. Therefore, the mix was designed to produce a highly flowable, high-strength, and well-compacted mortar suitable for casting the specimens. The mortar used for the plates was designed to achieve a compressive strength of 35 MPa after 28 days. A mechanical laboratory mixer was used to prepare the mixes. The materials were first dry mixed, after which water was added and the mixture was mixed again for each specimen. The proportions of the mortar mix per cubic meter are listed in Table 10. The compressive strength of the mix was experimentally evaluated in accordance with ISO 1920-3/2004. Three cube specimens measuring 150 mm × 150 mm × 150 mm were cast and tested in compression at curing ages of 7 and 28 days. The results are summarized in Table 11.

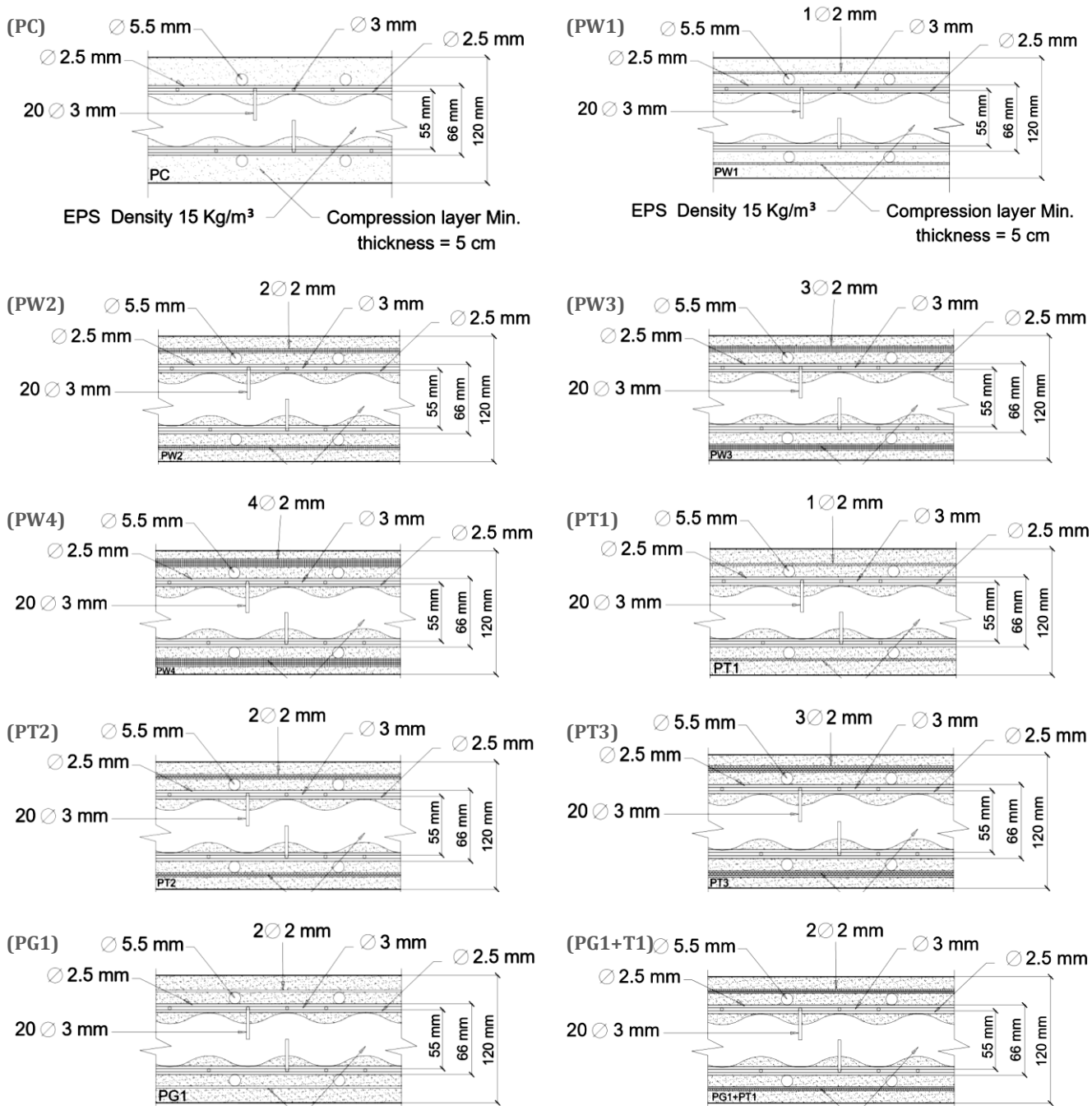

Fig. 11. Cross-sectional details of the tested plates.

Table 10. Mortar constituents for 1 m^3.

Constituent	Cement	Silica fume (kg)	Sand	Water	Superplasticizer (kg)	Fiber (e300) (kg)
Quantity (kg/m^3)	650	65	1250	240	14	1

Table 11. Compression test results.

Period (days)		7 days	28 days	Average compressive strength (MPa)
		Maximum compressive strength (MPa)		
Cubic specimen no.	1	21.2	37.3	35.1
	2	23.0	33.4	
	3	26.1	34.6	

3.2. Specimen fabrication and casting process

Wooden molds with the required dimensions were used to cast the specimens, as shown in Fig. 12. The welded steel bars, corrugated foam panels, and reinforcing meshes were assembled outside the molds according to the specified dimensions. The assembled reinforcement system was then placed inside the wooden mold before casting. After 24 hours, the specimens were demolded and cured with wet burlap for 7 consecutive days, as recommended by ECP 203/2020.

Fig. 12. Preparation, casting, and curing of the tested plates.

3.3. Test setup and instrumentation

After 28 days, the specimens were painted white to facilitate crack detection during testing. Rubber pads were placed between the plates and the testing device. The first cracking load, crack propagation, and failure mode of each specimen were recorded. Four demec points were positioned on one side of each specimen to measure strain during loading, as shown in Fig. 13. The experimental work was carried out in the Laboratory of Properties and Testing Materials, Faculty of Engineering, Menoufia University, Egypt.

Each specimen was placed in a universal testing machine with a maximum capacity of 200 kN. The tests were conducted using a four-line loading system, as illustrated in Fig. 13. The specimen was centered in the machine, and the distance between the two supports was maintained at 1100 mm. A dial gauge with an accuracy of 0.01 mm was positioned at mid-span under the specimen to measure deflection with increasing load, as shown in Fig. 14.

The load was applied in 5 kN increments using a load-control protocol. This increment was selected to provide a sufficient number of data points for accurately plotting the load-deflection curve, particularly in the pre-cracking and early post-cracking stages. It also enabled clear identification of the first cracking load while maintaining a manageable test duration. At each load increment, the horizontal distance between each pair of demec points was measured using a mechanical strain gauge reader, and the mid-span deflection was recorded using the dial gauge. Cracks were traced on the specimen sides and marked with a black marker. The load was gradually increased until complete failure occurred.

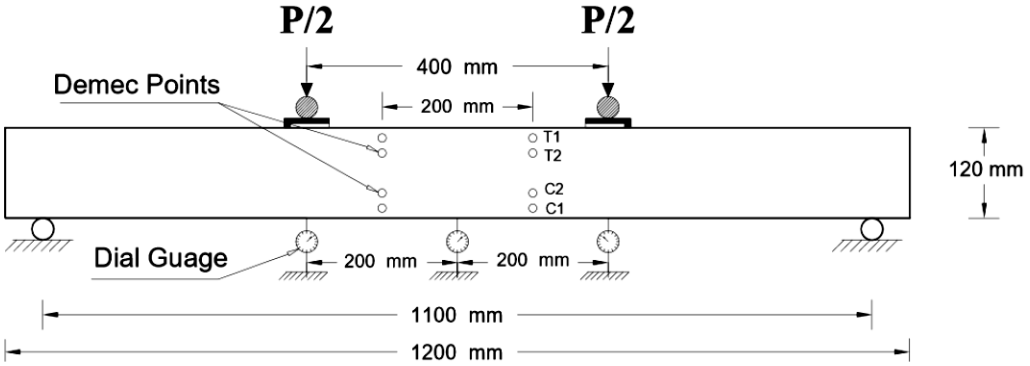

Fig. 13. Location of the demec points and dial gauges.

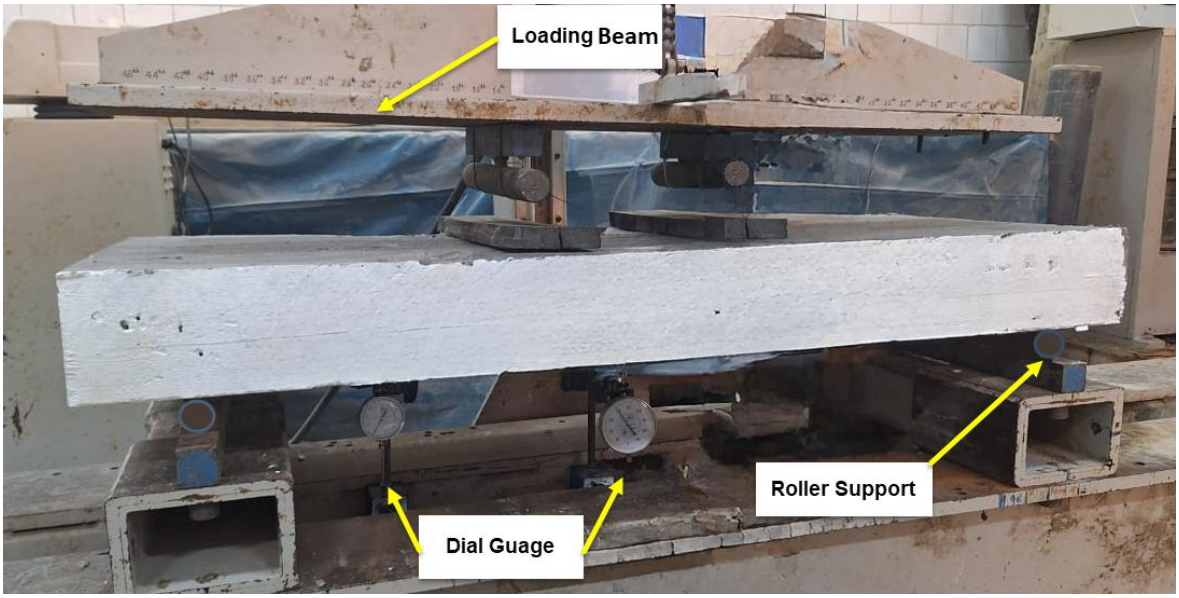

Fig. 14. Test setup.

4. Results and Discussion

4.1. Load-deflection relationship

Fig. 15 presents the load-deflection relationships for all tested plates, and Fig. 15(e) compares the responses of all groups. The control specimen (PC) had the lowest ultimate load (31.6 kN) and maximum deflection (11.22 mm). All reinforced plates exhibited higher strength and ductility than the control specimen. Group A (PW) showed a progressive increase in ultimate load from 35.2 to 52.3 kN as the number of welded mesh layers increased. Group B (PT) showed moderate improvement, with ultimate loads ranging from 40.7 to 46.2 kN. Group C (PG) achieved high performance, with specimen PG1+T1 reaching an ultimate load of 51.4 kN, confirming that the combined use of Tenax and Gavazzi meshes enhanced the ultimate strength.

The serviceability load was defined as the load corresponding to a mid-span deflection equal to the slab span divided by 250, as specified by ECP 203/2020. As summarized in Table 12, the control specimen (PC) exhibited a serviceability load of 11.3 kN. Specimens reinforced with welded and Tenax meshes showed significant increases in serviceability load, ranging from 13.63% to 97.10% for Group A and from 46.26% to 75.21% for Group B. The specimen reinforced only with Gavazzi mesh showed a slight increase of 3.41%, whereas the hybrid specimen (PG1+T1) exhibited a 66.64% increase.

The higher stiffness observed in specimens with welded wire mesh was directly associated with its high modulus of elasticity (E = 170 GPa) and proof strength (F_y = 400 MPa). This metallic reinforcement provides a rigid internal skeleton within the 120 mm plate, offering strong resistance to initial deformation in the linear elastic stage and maintaining the slope of the load-deflection curve before first cracking. Although welded mesh provided greater stiffness, Gavazzi mesh (E = 72 GPa, F_u = 325 MPa) was more flexible and had higher strain capacity.

4.2. Ductility ratio

The ductility ratio is defined as the ratio of the mid-span deflection at ultimate load (Δu) to the deflection at first cracking load (Δy). Therefore, the ductility ratio ($\Delta u/\Delta y$) represents the deformation capacity of the plate beyond first cracking. As shown in Table 12, the control plate (PC) exhibited the lowest ductility ratio (1.00). Plates reinforced with welded wire mesh (Group A) showed clear improvement, reaching a maximum value of 2.36 for specimen PW4. Tenax mesh plates (Group B) also showed improved ductility, with values ranging from 1.67 to 2.11. In contrast, the Gavazzi mesh plate (PG1) recorded the lowest ductility ratio (0.75), while the hybrid plate (PG1+T1) improved to 1.71. Overall, most reinforced plates exhibited higher ductility than the control specimen.

4.3. Energy absorption

Energy absorption (EA) was calculated as the area under the load-deflection curve for each plate. This area was obtained by integrating the applied load with respect to displacement from the beginning of loading to the displacement at failure. The trapezoidal numerical integration method was used to calculate the area according to Eq. (1).

$$EA = \sum_{i=1}^{n} \frac{F_i + F_{i+1}}{2} \Delta_{x_i} \quad (1)$$

As shown in Table 12, the control specimen (PC) absorbed 227.09 kN·mm, whereas all reinforced plates exhibited higher energy absorption. Specimens PG1 (398.98 kN·mm) and PG1+T1 (391.30 kN·mm) showed the highest values, indicating that non-metallic reinforcement meshes increased the energy absorption capacity of the plates compared with the control specimen. The use of Gavazzi and Tenax meshes improved energy absorption because their lower elastic modulus allowed greater deformation and, consequently, a larger area under the load-deflection curve. Overall, plates reinforced

with Tenax mesh (Group B) absorbed less energy than those reinforced with welded wire mesh (Group A), while Gavazzi and the hybrid mesh system provided the highest energy dissipation.

4.4. Concrete strain

Fig. 16 shows the load-strain curves for all tested plates. In general, increasing the number of reinforcement mesh layers increased the compressive strain because of the higher stiffness and load-carrying capacity of the plates. Specimen PW4 achieved the maximum compressive strain value (-0.00083). In contrast, the tensile strain on the concrete surface decreased as the number of reinforcement layers increased, indicating that the additional mesh layers helped reduce surface tensile deformation.

4.5. Cracking behavior

Fig. 17 shows the crack patterns for the different test groups. In all specimens, cracking began near the mid-span region. As the applied load increased, cracks propagated from the tension side toward the compression side and extended across the plate. The first cracking load varied according to mesh type, as shown in Table 12. With further loading, new cracks formed on both sides of the initial crack, while the first crack continued to propagate vertically. Additional cracks also developed as the load increased, although the earlier cracks mainly continued to grow vertically. The first cracking load was recorded during testing, and the flexural serviceability load was determined for each specimen, as listed in Table 12. Plates reinforced with welded mesh showed fewer but wider cracks, indicating a more localized and brittle failure once the steel yielded. In contrast, specimens reinforced with Gavazzi mesh (PG1) or with the Gavazzi-Tenax hybrid system (PG1+T1) exhibited a multi-cracking pattern with many fine and closely spaced cracks. This confirms that the Gavazzi mesh effectively arrested crack propagation and distributed energy across the plate span, thereby improving toughness and ductility. All specimens failed in flexure.

Table 12. Summary of results for all tested plates.

Specimen group	Specimen	First crack load (kN)	Ultimate load (kN)	Maximum deflection (mm)	Serviceability load (kN)	Ductility ratio Δ_u / Δ_y	Energy absorption (kN·mm)	Weight (kg)	Load / weight ratio (kN/kg)
Control	PC	8	31.6	11.22	11.3	1	227.09	135	0.23
A	PW1	10	35.2	11	12.8	1.16	259.15	136	0.26
	PW2	12	39.3	10.23	15.4	1.5	276.88	137	0.29
	PW3	13.5	42	9.98	16.8	1.69	294.1	138	0.30
	PW4	15	52.3	9.42	22.2	2.36	316.82	139	0.38
B	PT1	9	40.7	9.88	16.5	1.67	242.97	138	0.29
	PT2	11	44.4	9.43	18.8	2.00	240.52	139	0.32
	PT3	12.5	46.2	9.36	19.7	2.11	251.87	140	0.33
C	PG1	12	39.5	14.52	11.9	0.75	398.98	139	0.28
	PG1+T1	14	51.4	10.95	18.776	1.71	391.3	142	0.36

5. Conclusions

The following conclusions can be drawn from the experimental results and observations:

- Adding reinforcing mesh significantly improved ultimate load, service load, ductility, and energy absorption compared with the control plate (PC).
- Plates reinforced with welded mesh (Group A) increased the ultimate load by an average of 34% compared with PC.
- The plate reinforced with four layers of welded mesh (PW4) achieved the highest ultimate load (52.3 kN) and ductility ratio (2.36).
- The plate reinforced with one layer of Gavazzi mesh (PG1) achieved the highest energy absorption value (398.98 kN·mm), which was 75.9% higher than that of the control specimen.
- Service loads increased by 48.88% for PW4 and by 31.48% for PT3 compared with PC.
- The highest ductility ratios were obtained for PT3 and PW4, with improvements of 111% and 136%, respectively, compared with PC.
- The plate reinforced with four layers of welded mesh (PW4) achieved the highest load-to-weight ratio of 0.38 kN/kg, corresponding to an increase of more than 65% compared with the control plate. This indicates a higher load-carrying capacity for the same structural weight.

6. Recommendations

- Investigate the behavior of lightweight ferrocement plates reinforced with different meshes under impact and dynamic loading.
- Study the effect of high temperature and fire exposure on ultimate load, ductility, and energy absorption.
- Evaluate alternative mesh materials, such as polyethylene or geogrid systems, and their influence on strength and durability.
- Assess the acoustic performance of lightweight ferrocement plates used in building floors and walls.
- Conduct an economic study covering materials, fabrication, labor, and maintenance to evaluate cost-effectiveness.
- Investigate long-term durability under harsh environmental conditions, including moisture, chemicals, and temperature variations.

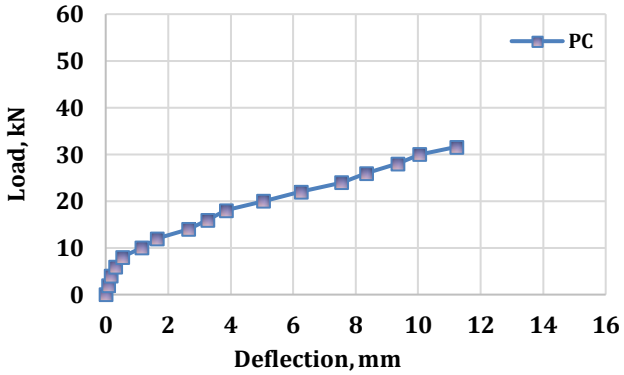

(a) Control plate

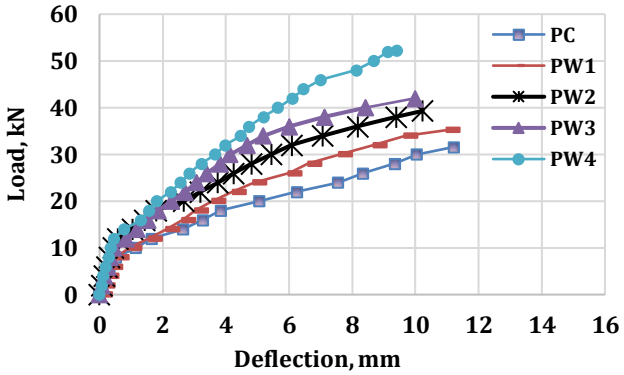

(b) Group A

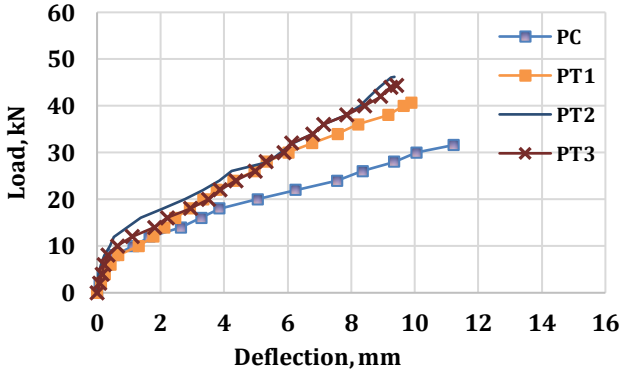

(c) Group B

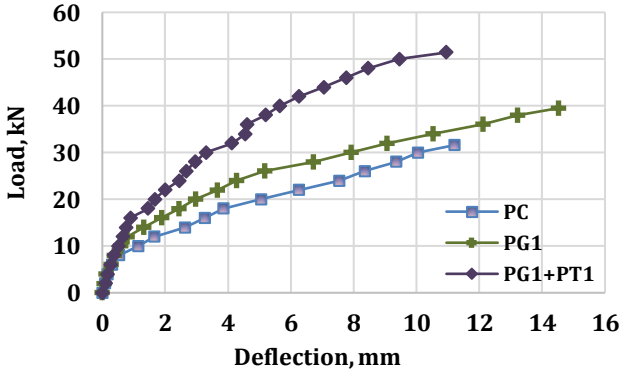

(d) Group C

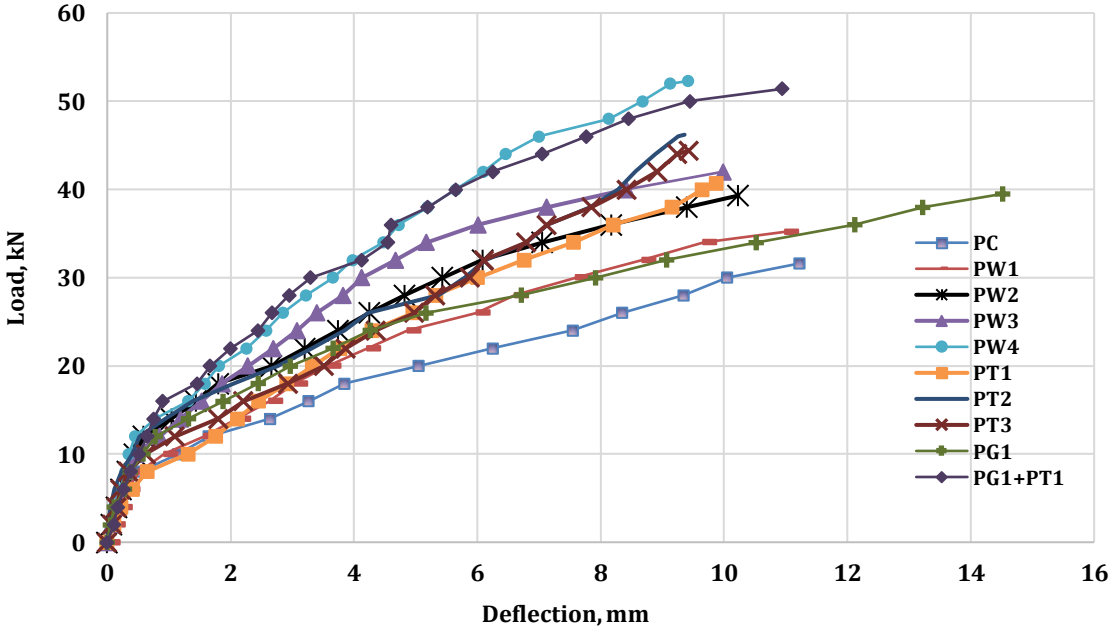

(e) All groups

Fig. 15. Load-deflection curves of different groups.

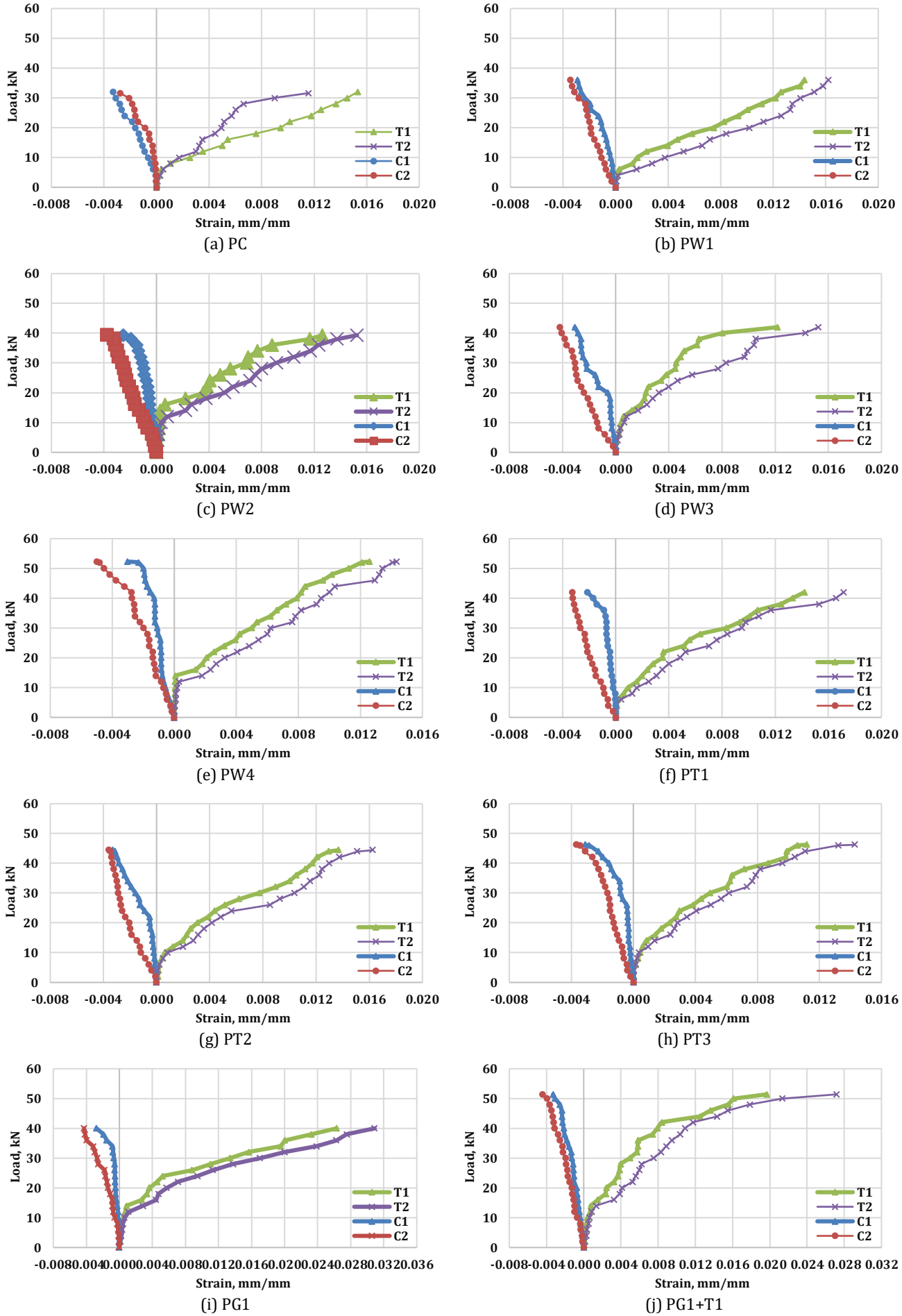

Fig. 16. Load-strain curves of different groups.

(a) PC

(b) PW1

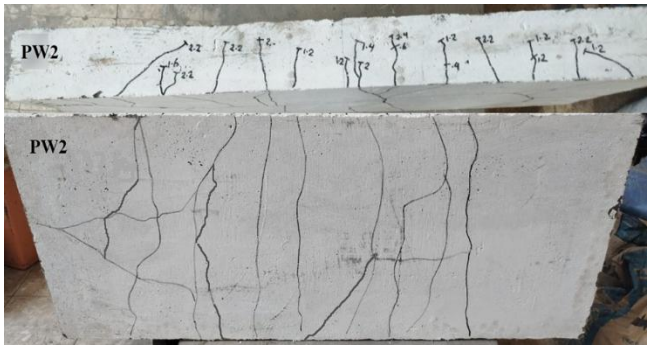

(c) PW2

(d) PW3

(e) PW4

(f) PT1

(g) PT2

(h) PT3

(i) PG1

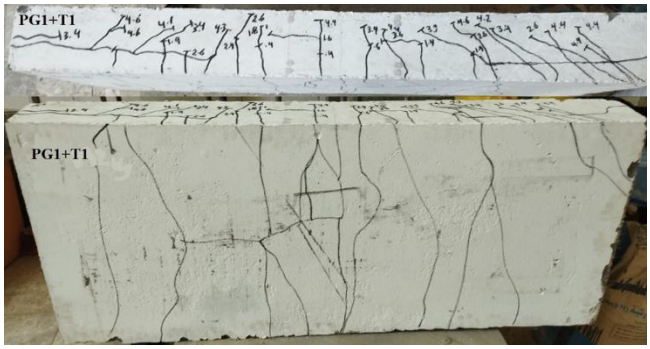

(j) PG1+T1

Fig. 17. Cracking patterns of different groups.

Acknowledgements

None declared.

Funding

The authors received no financial support for the research, authorship, and/or publication of this manuscript.

Conflict of Interest

The authors declare no potential conflicts of interest with respect to the research, authorship, and/or publication of this manuscript.

Data Availability

The datasets generated and/or analyzed during the current study are not publicly available but are available from the corresponding author upon reasonable request.

AI Assistance

No AI-based tools were used in the preparation of this manuscript.

Author Contributions

All authors made substantial contributions to the conception and design of the study, acquisition of data, analysis and interpretation of data; drafted or critically revised the manuscript for important intellectual content; and approved the final version to be published.

REFERENCES

Abdel Tawab A (2006). Development of Permanent Formwork for Beams Using Ferrocement Laminates. *Ph.D. thesis*, Menoufia University, Shebin El-Kom, Egypt.

Acma LMC, Dumpasan GC, Salva MI, Mansaguiton MP, Supremo RP, Daquiado NFP (2015). Flexural strength and ductility behavior of ferrocement I-beam. *Mindanao Journal of Science and Technology*, 13(1), 99-108.

Dawood ET, Shawkat AS, Abdullah MH (2021). Flexural performance of ferrocement based on sustainable high-performance mortar. *Case Studies in Construction Materials*, 15, e00566.

ECP 203/2020 (2020). Egyptian code of practice: Design and construction of reinforced concrete structures. Housing and Building National Research Center (HBRC), Cairo, Egypt.

El-Sayed TA, Deifalla AF, Shaheen YBI, Ahmed HH, Youssef AK (2023). Experimental and numerical studies on flexural behaviour of GGBS-based geopolymer ferrocement beams. *Civil Engineering Journal*, 9(3), 629-653.

Eltaly BA, Shaheen YBI, El-Boridy AT, Fayed S (2023). Ferrocement composite columns incorporating hollow core filled with lightweight concrete. *Engineering Structures*, 280, 115672.

EOS 1658-4 (2018). Testing hardened concrete. Part 4: Making and curing specimens for strength test. Egyptian Organization for Standardization and Quality (EOS), Cairo, Egypt.

ESS 1109 (2021). Aggregates for concrete. Egyptian Organization for Standardization and Quality (EOS), Cairo, Egypt.

ESS 4756-1 (2022). Cement. Part 1: Composition, specifications and conformity criteria for common cements. Egyptian Organization for Standardization and Quality (EOS), Cairo, Egypt.

ISO 1920-3 (2004). Testing of concrete. Part 3: Making and curing test specimens. International Organization for Standardization, Geneva, Switzerland.

Madadi A, Eskandari-Naddaf H, Shadnia R, Zhang L (2018). Digital image correlation to characterize the flexural behaviour of lightweight ferrocement slab panels. *Construction and Building Materials*, 189, 967-977.

Murali G, Amran M, Fediuk R, Vatin N, Raman SN, Maithreyi G, Sumathi A (2020). Structural behaviour of fibrous-ferrocement panel subjected to flexural and impact loads. *Materials*, 13(24), 5648.

Naveen GM, Suresh GS (2020). A study of fiber reinforced light weight ferrocement beams under monotonic and repeated loading. *International Research Journal of Engineering and Technology*, 7(12), 41-47.

Qureshi HJ, Khurram N, Akmal U, Arifuzzaman M, Habib Q, Al Fuhaid AF (2023). Flexure performance of ferrocement panels using SBR latex and polypropylene fibers with PVC and iron welded meshes. *Polymers*, 15(10), 2304.

Rajguru RS, Patkar M (2022). Torsion behaviour of strengthened RC beams by ferrocement. *Materials Today: Proceedings*, 61, 138-142.

Rao TC, Rao TG, Rao NR (2008). An experimental study on ferro cement channel units under flexural loading. *International Journal of Mechanics and Solids*, 3(2), 195-203.

Shaheen YBI, Soliman NM, Hafiz AM (2013). Structural behaviour of ferrocement channels beams. *Concrete Research Letters*, 4(3), 621-638.

Shaheen YBI, Nasser AA, El-Habashy WS (2016). Behaviour of ferrocement sandwich panels slabs under shear. *Concrete Research Letters*, 7(1), 11-23.

Shaheen YBI, Eltaly BA, Yousef SG, Fayed S (2023a). Structural performance of ferrocement beams incorporating longitudinal hole filled with lightweight concrete. *International Journal of Concrete Structures and Materials*, 17(1), 21.

Shaheen YBI, Etman ZA, Kandil DE (2023b). Performance of light weight ferrocement composite walls. *Challenge Journal of Concrete Research Letters*, 14(3), 110-125.

Shaheen YBI, Etman ZA, Mohamed AAF (2024). Structural behavior of ferrocement beams with circular openings. *Challenge Journal of Structural Mechanics*, 10(4), 116-137.